

## Parametric Analysis of the Closed-Water Activation Loop at the JSI TRIGA Reactor

Domen Kotnik<sup>1,2</sup>,

**Kristina Pahor<sup>1,2</sup>, Luka Snoj<sup>1,2</sup>, Igor Lengar<sup>2</sup>**

<sup>1</sup> Faculty of mathematics and physics, University of Ljubljana  
Jadranska 19, 1000 Ljubljana, Slovenia

<sup>2</sup> Reactor Physics Department, Jožef Stefan Institute  
Jamova cesta 39, 1000, Ljubljana, Slovenia  
domen.kotnik@ijs.si

kristina.pahor@student.fmf.uni-lj.si, luka.snoj@ijs.si, igor.lengar@ijs.si

### ABSTRACT

A unique, first of a kind, 6 MeV – 7 MeV gamma ray irradiation facility is being set up at the existing JSI TRIGA research reactor by installing a closed water loop for water activation. Special attention was devoted to the estimation and reduction of experimental uncertainties. Specifically, the detailed uncertainty and sensitivity study of the relevant parameters has been performed. The results show that one of the most important parameters is the ratio between irradiation time and overall transport time, as it greatly impacts the maximum saturation specific activity that can be achieved using a closed-water loop. On the other hand, water flow impacts the number of required loops to achieve saturation. Even though the flow rate differed by a factor of 10, resulting in 2 - 14 loops to reach the saturation value, the maximum saturation value didn't differ more than 20 % for all cases. Furthermore, all saturation values were reached after a similar time (roughly 42 s - 52 s, at the fixed total loop size of 8.5 m). Uncertainty and sensitivity analyses showed that, at shorter loop length, the highest impact on the total uncertainty of the specific activity has reaction rate and irradiation time, both contributing a constant uncertainty independently on the loop length. As the overall loop time/length increases the contribution of the isotope decay constant is starting to prevail and continuously, almost linearly increasing resulting in large total uncertainty. The impact of the latter can be reduced with higher water flow rates.

### 1 INTRODUCTION

Water as a primary coolant is being used in most of today's fission reactors and it is also one of the most promising coolants for future fusion reactors. During cooling of the reactor blanket (fusion) or cooling the reactor core (fission), the water is exposed to neutrons and gets activated, which leads to radioactive decay and release of high-energy gamma rays and neutrons. Many computational analyses of the water activation process have been performed for ITER [1] and DEMO [2]; however, results are subject to large uncertainties and consequently poor quality due to lack of experimental nuclear data, inaccurate computational methodologies/codes and lack of experimental facilities for experimental validation of methodology [3], [4]. Such large uncertainties in nuclear data could put the operation of ITER and DEMO at stake, as the dose rate due to activated water is estimated to be several 100 Sv/h for ITER and even larger for DEMO [5], [6]. In light of this, a water activation loop will be constructed at the Jožef Stefan Institute (JSI) TRIGA Mark II reactor [7]. The closed-water

activation loop will serve as a well-defined and stable 6 MeV – 7 MeV gamma-ray source. Furthermore, such a facility will enable various water activation-based experiments. They are essential to fill the knowledge gaps and to improve existing experimental nuclear data sets. This may greatly impact future fusion reactors, especially ITER and DEMO, as the optimisation of the amount of the required shielding material can lower the overall cost of the fusion device and make maintenance easier. Basic water activation experiments have previously been carried out also at the JSI TRIGA research reactor in Slovenia [8], [9].

The aim of the present work is estimation and reduction of experimental uncertainties to design a facility for performing benchmark experiments, e.g. calibration of detectors (HPGe, scintillation detectors, ionization chambers) and dosimeters (TLD), shielding experiments using ITER-like-wall materials (Eurofer, Nb<sub>3</sub>Sn, tungsten, beryllium, carbon, lead, heavy concrete), dose rates and gamma spectrum measurement along the water loop, integral cross-section measurements of oxygen isotopes, etc. For the optimal design of the water activation loop detailed uncertainty and sensitivity study of the most relevant parameters (e.g., irradiation time, loop time, transport time to the detector, reaction rates and decay constants) is presented. The paper is organized as follows. The principles of water activation and activity calculation are presented in the first part of the paper. In the second part, the proposed irradiation facility at the JSI TRIGA reactor using a closed-loop water circulation system, analysis and different loop configurations are presented. The last part of the paper consists of the detailed uncertainty and sensitivity study.

## 2 WATER ACTIVATION

Activation of cooling water predominantly consists of activation of oxygen isotopes via the  $^{16}\text{O}(n,p)^{16}\text{N}$ ,  $^{17}\text{O}(n,p)^{17}\text{N}$  and  $^{18}\text{O}(n,\gamma)^{19}\text{O}$  reactions [10], whereby the activation of dissolved gasses, corrosion products and additions have negligible contribution. Activated N and O nuclides subsequently decay by emitting various decay products (gamma rays and neutrons) with different energies. Reactions  $^{16}\text{O}(n,p)^{16}\text{N}$  and  $^{17}\text{O}(n,p)^{17}\text{N}$  are threshold reactions with energy thresholds at 10 MeV and 8 MeV respectively, whereby reaction  $^{18}\text{O}(n,\gamma)^{19}\text{O}$  takes place already at thermal energies. One of the main differences between fission and fusion reactors is the average energy of a neutron born, which is below 2 MeV for fission and 14 MeV for DT fusion. Thus, neutrons in fusion reactors induce water activity that is 5 orders of magnitude larger than in fission reactors of similar power. As the cooling water loop extends outside of the primary biological shield in fission/fusion reactors and distributes the radioactivity to many critical components, additional protection for detectors, instrumentation, superconducting coils, and personnel must be considered. It is important to note that radioactivity of the activated water is short-lived (order of seconds), hence it presents a radiation source only during reactor operation. The major contributors to the total water activity during operation are the activated oxygen nuclides, especially activated isotope  $^{16}\text{N}$  due to a high natural abundance of  $^{16}\text{O}$  for (n,p) reaction and high energy gamma radiation (6.13 MeV and 7.12 MeV). Due to this, the analyses presented in this paper are focused on the activation of this isotope [5].

### 2.1 Activity calculation

The change of specific activity  $a$  (activity per unit volume) of a nuclide, which is the result of the activation [11], is calculated as:

$$a(t) = R(1 - e^{-\lambda t_{irr}}), \quad (1)$$

where  $\lambda$  is a decay constant of the studied isotope,  $R$  is an average reaction rate in the region of interest and  $t_{irr}$  the irradiation time. After long exposure ( $t_{irr} \rightarrow \infty$ ), the activity reaches

saturation value  $a = R$ . To consider water transport through a pipe towards detector's position, i.e. specific activity after some transport time  $t_{trans}$ , additional decay term has to be applied to equation (1) as:

$$a(t) = R(1 - e^{-\lambda t_{irr}})e^{-\lambda t_{trans}}. \quad (2)$$

Furthermore, in the case of the closed-loop system, where water is circulating and is exposed to the neutron flux near the reactor core for a short period, the specific activity is increasing after each loop. Specific activities after the irradiation  $a_{outlet}$  and before the irradiation  $a_{inlet}$  are described as:

$$a_{outlet} = a_{inlet}e^{-\lambda t_{irr}} + R(1 - e^{-\lambda t_{irr}}) \quad \& \quad a_{inlet} = a_{outlet}e^{-\lambda T_{loop}} \quad (3)$$

where  $T_{loop}$  is transport time throughout the remaining pipe system from outlet to inlet. Therefore, the maximum specific activity at detector's position, which can be achieved with a closed-loop, is determined with the new equilibrium (saturation) value  $a_{sat}$  as:

$$a_{sat}(t) = \frac{R(1 - e^{-\lambda t_{irr}})e^{-\lambda t_{trans}}}{1 - e^{-\lambda(T_{loop} + t_{irr})}} = \frac{R(1 - e^{-\lambda t_{irr}})e^{-\lambda t_{trans}}}{1 - e^{-\lambda T_{tot}}}, \quad (4)$$

where  $T_{tot}$  is the total circulation time of the proposed closed-water loop system.

### 3 CLOSED-LOOP FOR WATER ACTIVATION AT JSI TRIGA REACTOR

The Jožef Stefan Institute TRIGA Mark II reactor (JSI TRIGA) is a 250 kW light water pool-type research reactor cooled by natural convection [7]. Irradiation channels are located in the outermost positions of the core with one extra channel at the central position of the reactor core. There are also three horizontal irradiation channels, i.e. two radial and one tangential, penetrating the concrete structure of the reactor. One of the radial ports ends on the outside of the graphite reflector while the other, namely the radial piercing port, penetrates the graphite reflector and reaches the reactor core. The latter port was therefore chosen as the main candidate for the installation of the closed-water loop due to the much higher neutron flux causing a higher activation rate of water. The schematic presentation of the JSI TRIGA reactor core is shown in Fig. 1 (left) in a horizontal cross-section view.

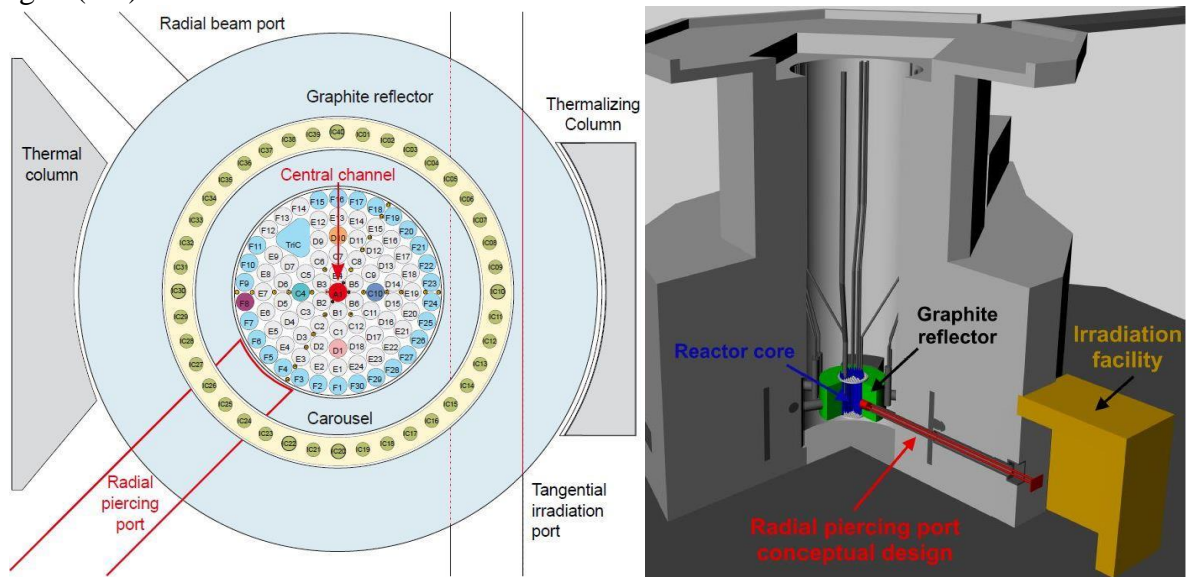


Figure 1: Scheme of the JSI TRIGA reactor core. Radial piercing port, shown in red, was chosen for the installation of the closed-water loop (left). Model of the basic conceptual design of the water activation loop in radial piercing port (right).

The basic conceptual design of the irradiation facility of the closed-loop for water activation, shown in Fig. 1 (right), consists of a pipe loop, which is inserted into the radial piercing port where the water is activated. The pipes with the activated water will be guided outside of the port directly to the irradiation facility next to the port opening (length of the pipe around 3.1 m). The previous analysis confirmed [12] that such configuration, using the radial piercing port, rather than utilizing the central irradiation channel where pipes would be guided through the reactor tank to the reactor platform and then back down to the ground floor (length of the pipes more than 15 m), would present the overall best option for the irradiation facility (e.g. simpler design, already present concrete biological shield around the loop and comparable  $^{16}\text{N}$  decay rates in the irradiation facility).

### 3.1 Activity analysis of different loop configurations

To determine the optimal design of the closed-loop for water activation, which will serve as an irradiation facility for performing various benchmark experiments, a study of different parameters and their dependence on the specific activity is of utmost importance. Based on Eq. (3 and 4), the main parameters, which are directly related to the water loop design, are the irradiation time and the total transport time throughout the entire loop. On the other hand, the reaction rate has a high linear impact on the specific activity, however, it isn't affected by the loop size but depends on the reaction cross-section for neutron activation of the related isotopes. To analyse the impact of the individual parameter, other parameters have to be predefined and unchanged during the analysis. For the upcoming analyses the length of the transport part of the loop  $L_{loop}$  (from the outlet to inlet with the absence of the irradiation part  $L_{irr}$ ) was set to 8.5 m of which approximately 6.2 m are fixed due to the radial piercing port dimensions<sup>1</sup>. In addition, the pipe diameter of 5 cm and constant water flow  $\Phi$  of 2 l/s was chosen, resulting in water velocity of roughly 1 m/s. Two detectors were placed at fixed positions along the loop, both 50 cm from the exit/entrance of the radial piercing port, resulting as a position 3.6 m after the irradiation part (detector 1) and 3.6 m before the irradiation part (detector 2), respectively. The scheme of the closed-water loop is shown in Fig. 2.

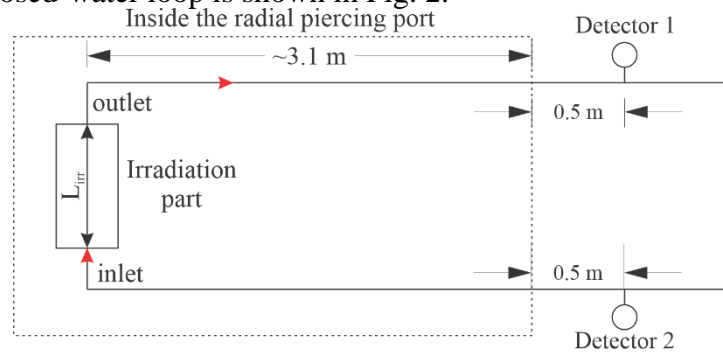


Figure 2: Scheme of the closed-water loop.

#### 3.1.1 Variation of the irradiation part of the water loop

For the first analysis the length of the irradiation part of the loop  $L_{irr}$ , which is the closest part near the reactor core, was artificially<sup>2</sup> varied from 20 cm to 100 cm. The first analysis, shown in Fig. 3, presents the specific activity of the  $^{16}\text{N}$  at the “detector 1” position in

<sup>1</sup> The length of the radial piercing port is approximately 3.1 m and to consider also additional shielding in front of the port entrance and part for the measurements, the minimum length of the  $L_{loop}$  must be at least 7.5 m.

<sup>2</sup> The design of the irradiation part is not yet known. The length can be shortened/extended based on the pipe winding.

dependence on time. The time axis extends until the value, when the activity reaches 99 % of the saturation value (see Eq. 4). Dotted lines connecting individual points act as an eye guide only. We can observe that for all cases, the 99 % of the saturated value was achieved after 6 loops. Furthermore, longer irradiation time, which at constant water flow corresponds to a longer irradiation part of the loop, results in a higher total specific activity.

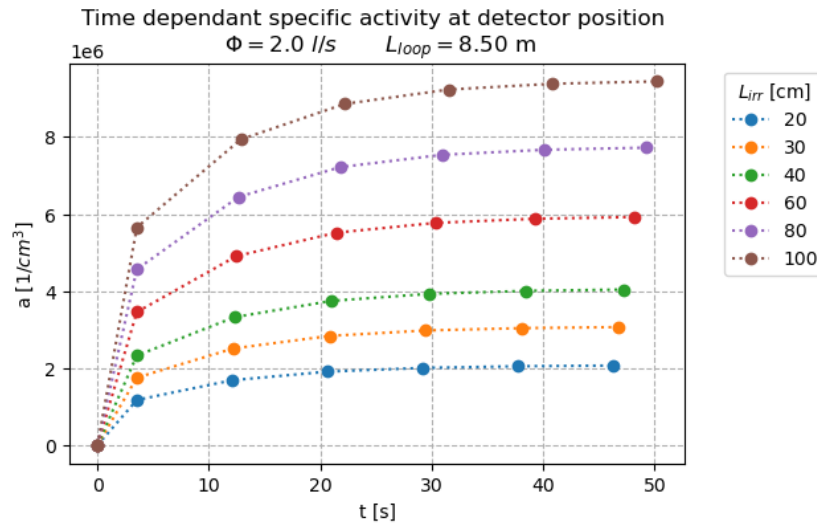


Figure 3: Specific activity of  $^{16}\text{N}$  at the “detector 1” position in dependence on time, time scale until activity reaches 99 % of the saturation value (after six loops) for 6 different lengths of the irradiation part of the loop (20 cm – 100 cm). Dot lines connecting points act as an eye guide only.

Specifically, at these predefined above-mentioned loop conditions, 5 times longer irradiation time leads to more than 4.5 times higher specific activity. Based on this, the length of the irradiation part has a large, almost linear, impact on the specific activity and therefore, special attention will be devoted to maximizing it.

### 3.1.2 Variation of the water flow rate

The second analysis consists of water flow rate variation, from 0.5 l/s to 5 l/s, whereby the irradiation part of the loop was set to 30 cm and the remaining part of the water loop was left unchanged at 8.5 m. In other words, varying the water flow rate at a fixed total water loop length, 8.8 m, results in different irradiation times ( $t_{irr}$ ) and total transport time ( $T_{tot}$ ) of the water. The specific activities of the  $^{16}\text{N}$  at the “detector 1” position (3.60 m distance after the irradiation part), in dependence on the time, scale up to 99 % of the saturation value, for 6 different water flow rates are shown in Fig. 4. We have to point out that the dot lines connecting individual points are shown for clarity only and don't represent the actual activity at that period of time. Results show that at the current loop configuration, using a water flow rate of 0.5 l/s would reach within 99 % of the saturation value already after the second loop. This was anticipated as in this case the total transport time throughout the loop system is almost 5 times longer than the half-life of the  $^{16}\text{N}$  resulting in a negligible role of having a closed-loop. By increasing the water flow rate, resulting in lower irradiation time and total transport time throughout the loop system, the saturation value is slightly increasing and at the same time, the number of loops is also increasing. At a certain point, somewhere between 1 l/s – 2 l/s, the maximum saturation activity is reached and then it starts slightly to decrease by further increasing the flow rate. This occurs as the irradiation time is getting lower and lower and therefore contribution from individual loops towards total activity is decreasing. Even though the flow rate differs by a factor of 10, resulting in 2 – 14 loops required to reach the saturation value, the maximum saturation value does not differ by more than 20 % for all cases. Furthermore, all saturation values are reached after a similar period (42 s – 52 s).

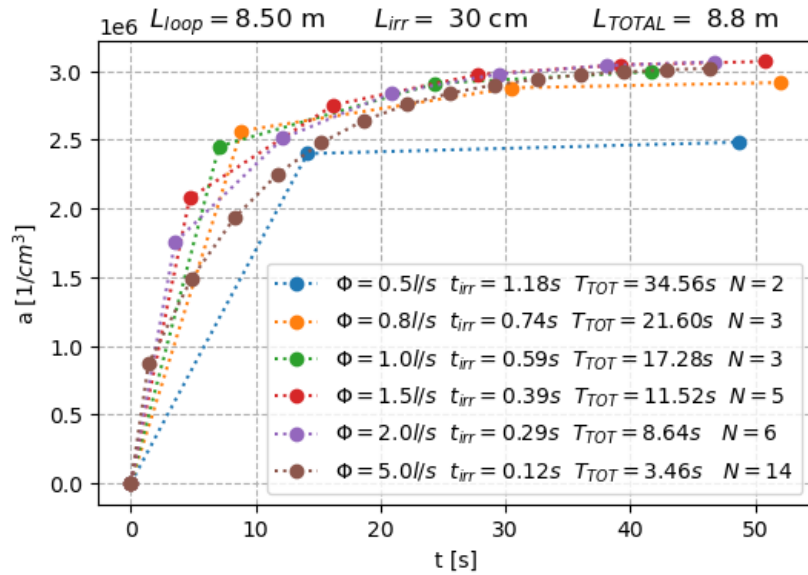


Figure 4: Specific activity of  $^{16}\text{N}$  at the “detector 1” position in dependence on the time after start of irradiation, time scale until 99 % of the saturation value. 6 different water flow rates (0.5 l/s – 5 l/s). Dot lines connecting individual points are shown for clarity only.

#### 4 UNCERTAINTY AND SENSITIVITY STUDY

In addition to the results obtained either by measurements or by various simulations, it is necessary to know the uncertainty of the results as it indicates their quality. Uncertainty indicates the dispersion of values that can be attributed with a certain probability to the measured or simulated quantity and consequently describes how reliable the result is. In light of this, an uncertainty and sensitivity study of the most relevant parameters, e.g. reaction rate, decay constant, irradiation time, transport time towards detector’s position and loop transport time (from the outlet to inlet with the absence of the irradiation part), was performed. In case of uncorrelated or unrelated data ( $X_1, X_2, \dots, X_N$ ) with uncertainties ( $\sigma_1, \sigma_2, \dots, \sigma_N$ ), then the uncertainty  $\sigma_f(X_1, X_2, \dots, X_N)$  of a function  $f(X_1, X_2, \dots, X_N)$  is defined as:

$$\sigma_f(X_1, X_2, \dots, X_N) = \sqrt{\sum_{i=1}^N \left( \sigma_i \frac{\partial f}{\partial X_i} \right)^2}. \quad (5)$$

Eq. (5) is a simplified form where it is assumed that the change of function  $f$  is linearly dependent on  $X$ . Such assumption is appropriate as the correlations between parameters are reasonably low or practically 0 and therefore the 2<sup>nd</sup> order term is negligible; for example: decay constant  $\lambda$  is isotope dependent and has non-correlation with the measurement of the loop transport time, which is determined by length and water flow rate. Based on the Eq. (4) and (5) the uncertainty of the equilibrium (saturation) value of the specific activity at the “detector 2” position (50 cm before the entrance to the radial piercing port or 3.60 m from the back end of the closed-loop)  $\sigma_{a_{sat}}$  is calculated as

$$\sigma_{a_{sat}} = \sqrt{\left( \sigma_R \frac{\partial a_0}{\partial R} \right)^2 + \left( \sigma_\lambda \frac{\partial a_0}{\partial \lambda} \right)^2 + \left( \sigma_{t_{irr}} \frac{\partial a_0}{\partial t_{irr}} \right)^2 + \left( \sigma_{t_{trans}} \frac{\partial a_0}{\partial t_{trans}} \right)^2 + \left( \sigma_T \frac{\partial a_0}{\partial T_{loop}} \right)^2}. \quad (6)$$

Results of the calculated uncertainties of the saturated specific activity at the “detector 2” position are shown in Fig. 5 for two water flow rates, 1.5 l/s (upper) and 5 l/s (lower) in

dependence on the loop transport time  $T_{loop}$  with a fixed loop irradiation part ( $L_{irr} = 30$  cm). Due to clarity, additional y-axis is shown, which corresponds to water loop size  $L_{loop}$  (from 8.5 m to 48.5 m). The graphs show with different colours absolute (left) and relative (right) uncertainties for the individual case when the uncertainty of only that particular parameter has been considered. Due to clarity and easier comparison between individual parameter's contribution to the total uncertainty, the relative uncertainty of all parameters (e.g.  $\frac{\sigma_R}{R}$ ,  $\frac{\sigma_{t_{irr}}}{t_{irr}}$ , ... etc.) was set to 10 %. In addition to the uncertainties for individual parameters separately, the black dashed line represents the overall uncertainty  $\sigma_{a_0}$ . Graph of the relative uncertainties clearly shows that parameters *reaction rate*, *irradiation time* and *transport time to detector* contributes constant uncertainty throughout the problem, whereby the impact of the transport time to detector is decreasing at higher water flow rates.

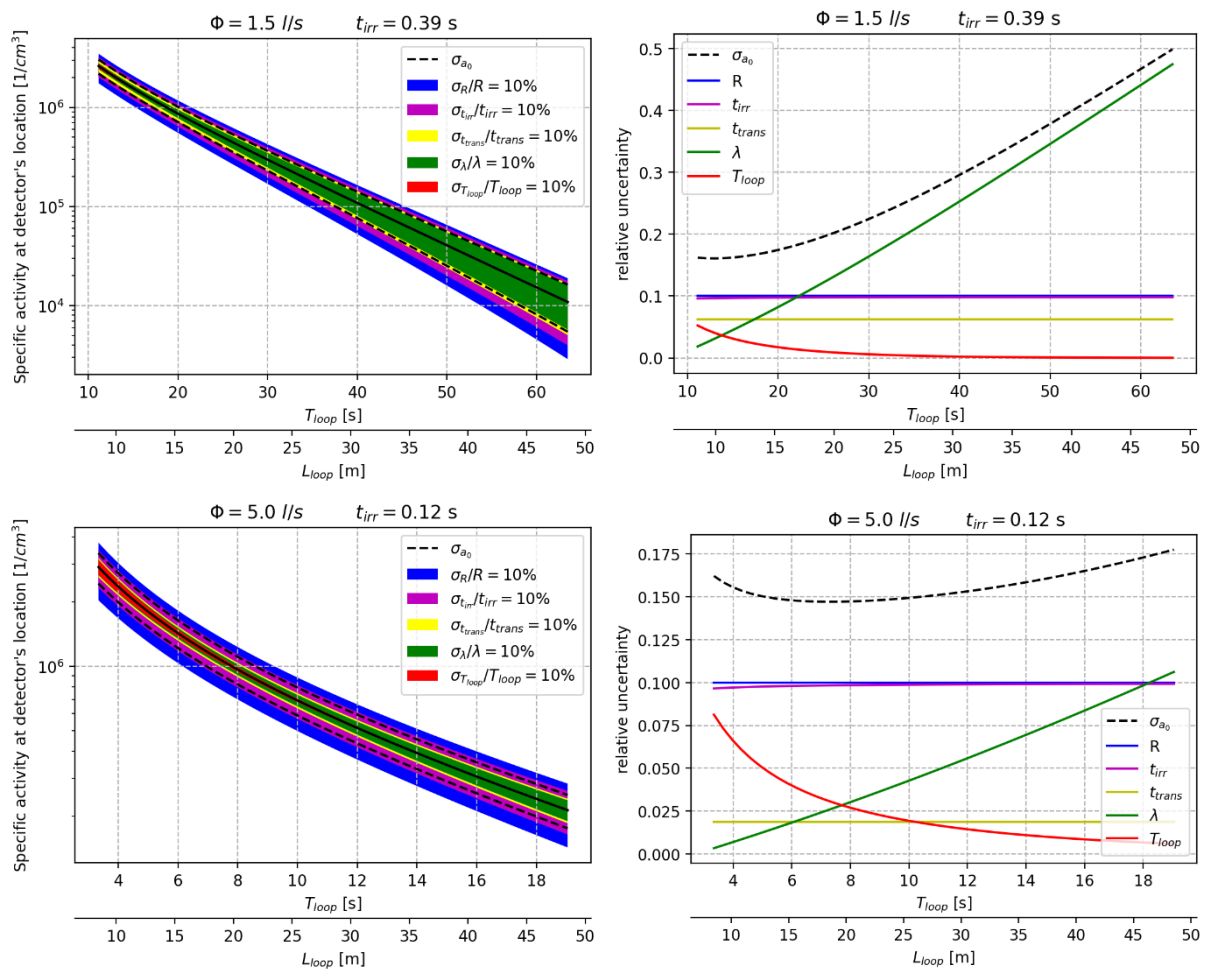


Figure 5: Uncertainty (left) and sensitivity (right) study of the specific activity at “detector 2” location in dependence on the loop transport time for two water flow rates (0.5 l/s and 5 l/s). Due to clarity, additional y-axis is shown, that corresponds to water loop size. The relative uncertainty of all studied parameters was set to 10 %.

Furthermore, the impact of the *overall loop time* is expectedly largest at shortest loop configurations and is then decreasing as the overall loop time is increased. The largest impact on the overall uncertainty has the *decay* constant parameter. At flow rate 1.5 l/s (upper right figure) it started to prevail and furtherly increasing at around 22 s of the loop time, which corresponds to the loop length, with the absence of the irradiation part, of approximately 16.5 m. At this point the total uncertainty is around 18 % and it reaches almost 50 % at the loop length of 48.5 m. However, by increasing the water flow rate (bottom right figure) its overall impact decreases. At flow rate 5 l/s, its impact is almost 4 times smaller compared at a flow rate

of 1.5 l/s. We have to point out that the mentioned analysis is highly conservative as 10 % of the relative uncertainty was assumed, due to better clarity, for all parameters.

## 5 CONCLUSION

The problem of water activation is currently dealing with a vast number of common flaws: large discrepancies and inconsistency between nuclear data libraries, lack of calculation tools/methodologies for dose rate calculations and on top of all, lack of experimental facilities featuring high energy gamma ray sources for shielding experiments around activated water. A unique 6 MeV – 7 MeV irradiation facility, which will involve a closed-loop for water activation, is being set up at the JSI TRIGA research reactor.

The impact of different loop design parameters was determined and uncertainty and sensitivity study were performed in order to get a deeper knowledge and to design a facility for performing benchmark experiments. Results show that one of the most important parameters is the irradiation time. Specifically, at predefined loop characteristics, 5 times longer irradiation time leads to more than 4.5 times higher specific saturated activity. It turned out that water flow rate has relatively low impact on the overall specific activity and 99 % of the saturation value has been achieved after a similar period of time. However, the main difference between cases was the required number of the loops. Results of the calculated uncertainties of the saturated specific activity at detector's position showed that the largest impact has the isotope decay constant with the increasing contribution as the overall loop time increases. Its impact decreases almost linearly at higher water flow rate; specifically, for a factor of 4 at a flow rate 5 l/s compared to the case with the flow rate of 1.5 l/s.

The performed uncertainty and sensitivity analysis will serve to provide guidance and better knowledge the length of the pipe-loop, the required water flow rate and how precisely we will need to know the experimental parameters of the device in order to be able to perform the measurements with a certain accuracy.

## ACKNOWLEDGMENTS

The authors acknowledge the support of the Slovenian Ministry of Education, Science and Sport (project codes P2-0405 Fusion technologies; P2-0073 Reactor physics; PR-09769 Training of young researchers).

## REFERENCES

- [1] ITER website, <https://www.iter.org>
- [2] EUROfusion, <http://www.euro-fusion.org/eurofusion/roadmap>, November 2018.
- [3] G. Zamir et al., (2015). Radiation levels in the ITER tokamak complex during and after plasma operation. *Fusion Engineering and Design*, 261-264. doi:101016/jfusengdes201505019.
- [4] P. Chiovaro, et al., Investigation of the DEMO WCLL Breeding Blanket Cooling Water Activation, *Fusion Engineering and Design*, Volume 157, 2020, 111697, ISSN 0920-3796.
- [5] Žohar A., Snoj L., On the dose fields due to activated cooling water in nuclear facilities, *Progress in Nuclear Energy*, Volume 117, 2019, 103042, ISSN 0149-1970.
- [6] Žohar A., et al., Analysis of water activation in fusion and fission nuclear facilities, *Fusion Engineering and Design*, Volume 160, 2020, 111828, ISSN 0920-3796.
- [7] A R. Jeraj and M. Ravnik, U(20)-Zirconium Hydride Fuel Rods in Water with Graphite Reflector, *International Handbook of Evaluated Criticality Safety Benchmark Experiments*, NEA/NSC/DOC(95)03, OECD-NEA, 2010.
- [8] Žohar A., et al., Analysis of irradiation experiments with activated water radiation source at the JSI TRIGA Research Reactor, *Fusion Engineering and Design*, Volume 161, 2020, 111946.
- [9] Žohar A., et al., Water Activation Experiments and Calculations at JSI TRIGA Research Reactor, NENE, 2020
- [10] D. Brown, et al., ENDF/B-VIII.0: The 8th Major Release of the Nuclear Reaction Data Library with CIELO-project Cross Sections, New Standards and Thermal Scattering Data, *Nuclear Data Sheets*, 2018.
- [11] Matjaž Stepišnik, Analiza aktivnosti primarnega hladila pri delovanju raziskovalnega reaktorja TRIGA MARK II, Magistrsko delo, 2008.
- [12] A. Žohar, et al., Conceptual Design of Irradiation Facility with 6 MeV and 7 MeV Gamma Rays at the JSI TRIGA Mark II Research Reactor, *EPJ Web Conf.* 225 04014 (2020).